JOURNAL OF COMPUTATIONAL PHYSICS 74, 177–190 (1988)

Solution of a Rotating Navier–Stokes Problem by a Nonlinear Multigrid Algorithm

GUY LONSDALE*

Department of Mathematics, University of Manchester, Manchester M13 9PL, United Kingdom

Received June 27, 1986; revised February 20, 1987

A full approximation scheme (FAS), nonlinear multigrid algorithm is considered for the solution of the incompressible steady-state Navier–Stokes and continuity equations in a rotating cylindrical-polar coordinate system; the specific problem being that of laminar source-sink flow between corotating discs. The pressure correction iteration is analysed as a smoother of the momentum and continuity equations, and an extended pressure correction scheme, modified for this problem, is used as the smoother for the multigrid algorithm. Also used are sequences of nonuniform, staggered grids for the primitive variables. Results are given for rotational Reynolds numbers in the range $2 \cdot 5 \times 10^3$–$2 \cdot 5 \times 10^4$ and the performance of the nonlinear multigrid algorithm is compared with that of the extended pressure correction method and also to the performance of the same pressure correction method incorporating a multigrid algorithm as a linear solver.

1. INTRODUCTION

In this paper we consider the solution of a simplified version of a problem in gas turbine design, the flow of air between rotating discs, by a nonlinear multigrid algorithm. The problem considered is that of laminar source-sink flow between corotating discs as in Chew [3] and Lonsdale and Walsh [7], where the solution procedure was a one-grid pressure correction method with various modifications to improve on the convergence rate.

A cylindrical-polar coordinate system (r, ϑ, z) rotating at angular velocity Ω (in the ϑ-direction) is used with variables and parameters as follows:

radial velocity	—	u
tangential velocity	—	v
axial velocity	—	w
pressure	—	p
density	—	ρ, assumed constant
reduced pressure	—	$p' = p - \frac{1}{2}\rho\Omega^2 r^2$

* Current address: School of Studies in Mathematical Sciences, University of Bradford, Bradford, West Yorkshire, BD7 1DP, United Kingdom

0021-9991/88 $3.00

dynamic viscosity — μ, assumed constant
source flow rate — Q
radial position of source — a
radial position of sink — b
distance between the discs — s.

The incompressible steady-state Navier–Stokes and continuity equations are then:

$$\frac{1}{r}\frac{\partial}{\partial r}(\rho r u^2)+\frac{\partial}{\partial z}(\rho u w)=-\frac{\partial p'}{\partial r}+\mu\left[\frac{1}{r}\frac{\partial}{\partial r}\left(r\frac{\partial u}{\partial r}\right)+\frac{\partial^2 u}{\partial z^2}-\frac{u}{r^2}\right]+2\rho\Omega v+\rho\frac{v^2}{r}, \quad (1)$$

$$\frac{1}{r}\frac{\partial}{\partial r}(\rho r u v)+\frac{\partial}{\partial z}(\rho v w)=\mu\left[\frac{1}{r}\frac{\partial}{\partial r}\left(r\frac{\partial v}{\partial r}\right)+\frac{\partial^2 v}{\partial z^2}-\frac{v}{r^2}\right]-\rho\frac{uv}{r}-2\rho\Omega u, \quad (2)$$

$$\frac{1}{r}\frac{\partial}{\partial r}(\rho r u w)+\frac{\partial}{\partial z}(\rho w^2)=-\frac{\partial p'}{\partial z}+\mu\left[\frac{1}{r}\frac{\partial}{\partial r}\left(r\frac{\partial w}{\partial r}\right)+\frac{\partial^2 w}{\partial z^2}\right], \quad (3)$$

$$\frac{1}{r}\frac{\partial}{\partial r}(ru)+\frac{\partial w}{\partial z}=0. \quad (4)$$

Boundary conditions for velicities are taken as follows:

$$u=\frac{Q}{2\pi r s}, \qquad v=0,\ w=0 \text{ at } r=a,\ b;$$

$$u=v=w=0 \qquad \text{at } z=0,\ s.$$

In the relaxation scheme used we require conditions only for a correction to the pressure, pp, not for the pressure itself (see Section 3); these conditions are taken to be:

$$\frac{\partial pp}{\partial r}=0 \qquad \text{at } r=a,\ b;$$

$$\frac{\partial pp}{\partial z}=0 \qquad \text{at } z=0,\ s.$$

The geometry and fluid properties used for numerical tests are as follows:

source radius, $a=0.019\text{m}$;
sink radius, $b=0.19\text{m}$;
distance between the discs, $s=0.0507\text{m}$;
constant dynamic vicosity, $\mu=1.78\times10^{-5}\text{kg/ms}$;
constant density, $\rho=1.225\text{kg/m}^3$;
source flow rate, $Q=2.761\times10^{-4}m^3/s$.

In order to solve the differential equations (1)–(4) numerically we first discretise the equations—covering the region by rectangular, possibly nonuniform, grids and representing the solution by values at the grid points. Note, however, that the velocities and pressure need not be calculated on coincident grids; the locations of velocities and pressure may be shifted or "staggered." In fact we use staggered grids throughout, with the velocities at points halfway between pressure lines as in Lonsdale and Walsh [7]. The use of staggered grids is discussed in detail in [9].

The finite difference equations may be found by integration over control areas (Varga [15]), and we use a further approximation in the assumption of linear profiles along control area boundaries.

For high Reynolds number flows it is necessary to use some form of upwind differencing for the convective terms [2, 9]. In this paper, the finite difference replacement of the momentum equations (1)–(3) includes the form of upwinding used by Patankar and Spalding [10] and discussed in detail in [9].

Discretisation of the differential equation in this way produces a nonlinear, coupled system of algebraic equations for the velocities and pressure at their respective grid points.

2. Multigrid Solution of a System of Nonlinear Algebraic Equations

The discretization of the Navier–Stokes and continuity equations leads to a nonlinear algebraic system of equations, as discussed in Section 1, so we first consider the major features of a multigrid solution of such a system. For a complete description of multigrid ideas and algorithms see Stüben and Trottenberg [11] or Brandt [1].

Let the nonlinear system be

$$\mathbf{N}_h(\mathbf{x}_h) = \mathbf{f}_h \qquad (R_h), \tag{5}$$

where

R_h is the fine, possibly staggered, grid;

$G(R_h)$ is the space of vectors of grid functions on R_h;

$\mathbf{x}_h, \mathbf{f}_h \in G(R_h)$;

we assume that a solution of (5) exists, so that

$$\mathbf{N}_h \text{ has an inverse.}$$

To develop a multigrid algorithm for this system we use the full approximation scheme (FAS):

If $\mathbf{x}_h^j$ is our current approximation to the solution $\mathbf{x}_h$, then the defect equation on the fine grid is

$$\mathbf{N}_h(\mathbf{x}_h^j + \mathbf{y}_h^j) - \mathbf{N}_h(\mathbf{x}_h^j) = \mathbf{d}_h^j, \tag{6}$$

where

$$\mathbf{d}_h^j = \mathbf{f}_h - \mathbf{N}_h(\mathbf{x}_h^j) \tag{7}$$

and the solution is given by $\mathbf{x}_h = \mathbf{x}_h^j + \mathbf{y}_h^j$. This gives us the coarse grid equation

$$\mathbf{N}_H(\mathbf{z}_H^j) = \mathbf{N}_H(\mathbf{x}_H^j) + \mathbf{d}_H^j, \tag{8}$$

where $\mathbf{z}_H^j = \mathbf{x}_H^j + \hat{\mathbf{y}}_H^j$, $\dim(G(R_H)) \ll \dim(G(R_h))$ and we assume $\mathbf{N}_H^{-1}$ exists.

In order to represent the defect equation (6) on the coarser grid it must first be smoothed by some relaxation process. As the system (5) is nonlinear the relaxation process will involve some linearisation; in fact, this linearisation need only be local to a point or line depending on the relaxation process used (see Section 3). The linearisation occurring in the relaxation process is the *only* linearisation required in the multigrid solution of Eq. (5). The defect (7) is calculated using the full nonlinear operator and we maintain a nonlinear system of equations on all grids. We can thus hope for fast, efficient convergence provided we can obtain a suitable relaxation method.

3. Relaxation Methods for the Navier-Stokes and continuity Equations

In this section we will discuss possibilities for the relaxation of the discretised Navier–Stokes and continuity equations. The methods we consider involve treating the momentum equations separately from the continuity equation so that the relaxation process is made up of two steps.

The handling of the momentum equations is quite standard, they are uncoupled via a linearisation which replaces products of variables with the product of one "old" iterate with one "new" iterate leading to five-point difference equations for the velocities. The momentum equations can thus be relaxed successively using either point or line relaxation methods such as Gauss–Seidel (in fact, we use the alternating line Gauss–Seidel algorithm). We note that this linearisation is not done globally before the relaxation sweeps for the momentum equations, but locally as required by the relaxation process.

The main problem in designing a relaxation method for the whole system lies in the handling of the continuity equation. Brandt and Dinar [2] introduce the idea of a "distributive relaxation," where changes are made to several variables in order to smooth the defect of an equation. The crucial factor in using a distributive relaxation to smooth the defect of the continuity equation is that changes made to the variables in order to satisfy continuity must not affect the smoothness already present in the momentum equations (in the sense of the defects of the linearised momentum equations).

We will first consider the distributive scheme proposed by Brandt and Dinar [2] and generalised by Fuchs and Zhao [4], for the Navier–Stokes equations in a car-

tesian coordinate system. This is most easily described in terms of the differential equations in the linearised form

$$Q^k \mathbf{u} + \nabla p = \mathbf{F}$$
$$\nabla \cdot \mathbf{u} = 0$$

where $Q^k = \rho \mathbf{u}^k \cdot \nabla - \mu \nabla^2$, $\mathbf{u}^k$ being our last iterate.

Let $\mathbf{u}^*$ be the velocities produced by smoothing the momentum equations with pressure p^k, giving a defect $\mathbf{d}^*$:

$$\mathbf{d}^* = \mathbf{F} - Q^k \mathbf{u}^* - \nabla p^k.$$

The distributive relaxation aims to produce new iterates $\mathbf{u}^{k+1}$ and p^{k+1} given by $\mathbf{u}^{k+1} = \mathbf{u}^* + \delta \mathbf{u}$, $p^{k+1} = p^k + pp$, such that the continuity equation is satisfied and the momentum defect remains unchanged, i.e.,

$$\mathbf{d}^{k+1} = \mathbf{F} - Q^k \mathbf{u}^{k+1} - \nabla p^{k+1} = \mathbf{d}^*, \tag{9}$$

$$\nabla \cdot \mathbf{u}^{k+1} = 0. \tag{10}$$

The scheme used by Fuchs and Zhao [4] uses changes given by the following:

$$\delta \mathbf{u} = \nabla \chi, \qquad pp = -Q^k \chi, \tag{11}$$

where χ is given by the solution of

$$\nabla^2 \chi = -\nabla \cdot \mathbf{u}^*.$$

The distributive Gauss–Seidel scheme used by Brandt and Dinar [2] is a particular case of the above where χ is restricted to being nonvanishing only at a point. The changes (11) satisfy Eqs. (9) and (10) under the assumption that Q^k, ∇ commute.

For the simplified case of the Stokes equation, with vanishing Reynolds number, Q^k is just given by $-\nabla^2$ and the change to the defects of the momentum equations is given by

$$(\nabla^2 - \nabla\nabla.)\, \nabla \chi$$

which is identically zero. However, we must remember that in practice we will be dealing with the discretised equations. Let us consider the specific example of the scheme used by Brandt and Dinar [2], with χ restricted to being nonzero at a point, for the case of the Stokes equations in a cylindrical-polar coordinate system with a uniform grid. It can be shown that the changes given by the discrete forms of Eq. (11) only maintain the defects of the momentum equations in the limit as the mesh size goes to zero (Lonsdale [8]). We note here that in a cartesian coordinate system the changes made by the discrete forms of (11) maintain the momentum defects exactly.

For a nonvanishing Reynolds number the commutativity of Q^k, ∇ is clearly not true in general, so that the momentum defects are only approximately maintained by the changes (11).

We now propose an alternative smoother for the continuity equation, the extended pressure correction scheme of Van Doormaal and Raithby [12] which gave the best performance of several pressure correction schemes for the rotating discs problem (Lonsdale and Walsh [7]).

In order to describe Van Doormaal and Raithby's scheme we will consider the discretised, linearised equations

$$Q_h^k \mathbf{u}_h = -\nabla_h p_h + \mathbf{F}_h, \tag{12}$$

$$\nabla_{\cdot h} \mathbf{u}_h = 0, \tag{13}$$

where Q_h^k, ∇_h, $\nabla_{\cdot h}$ are discrete forms of the operators $Q^k, \nabla, \nabla\cdot$ and $\mathbf{u}_h$, p_h represents values of the variables at grid points.

Let $Q_h^k = D_h + \tilde{Q}_h$, where D_h is the diagonal of the matrix Q_h^k and define $\tilde{D}_h$ by

$$\tilde{D}_h = \text{diag}(\tilde{d}_i) \text{ with } \tilde{d}_i = \sum_j \tilde{q}_{ij}$$

($\tilde{q}_{ij}$ being the $(i,j)^{\text{th}}$ element of the matrix $\tilde{Q}_h$).

The basic idea of all the pressure correction schemes is that a correction to pressure is calculated which, together with approximate velocity–pressure gradient relations, aims to satisfy both the continuity and momentum equations; that is to say, we make changes to satisfy the continuity equation while aiming to leave the momentum defects unchanged–the motivation for a distributive relaxation.

Van Doormaal and Raithby's scheme is given by $\mathbf{u}_h^{k+1} = \mathbf{u}^*{}_h + \delta\mathbf{u}_h$, $p_h^{k+1} = p_h^k + pp_h$:

$$\delta\mathbf{u}_h = -(D_h + \tilde{D}_h)^{-1} \nabla_h pp_h, \tag{14}$$

where pp_h is given by the solution of the pressure correction equation

$$\nabla_{\cdot h}(D_h + \tilde{D}_h)^{-1} \nabla_h pp_h = \nabla_{\cdot h} \mathbf{u}_h^*. \tag{15}$$

The changes given by (14) and (15) satisfy the continuity equation (13) while giving changes to the defects of the momentum equations given by

$$\mathbf{d}_h^{k+1} = \mathbf{d}_h^* + (Q_h^k (D_h + \tilde{D}_h)^{-1} - I) \nabla_h pp_h,$$

where I is the identity matrix.

Thus Van Doormaal and Raithby's extended pressure correction scheme satisfies continuity while approximately maintaining the momentum defects, just as they are only approximately maintained by the scheme given by the changes (11).

There are, however, advantages in using the pressure correction scheme, as follows:

(a) We can take account of situations, like the rotating discs problem with a rotating frame of reference, when the body forces **F** include terms dependent on the variables (in the rotating discs problem these may be the dominant terms in the equations, Lonsdale and Walsh [7]) by including the terms in our approximation to the inverse of the discrete form of the differential operator for each equation. The form of the finite difference equations including the handling of the body forces is given in [3].

(b) The use of a nonuniform grid further violates the commutativity of Q_h^k and ∇_h required by the discrete form of the scheme given by Eqs. (11). This is true even for the Stokes equaton in a cartesian coordinate system, just as the involvement of the radial variable in a cylindrical-polar coordinate system prevents the exact maintenance of the momentum defects (Lonsdale [8]). In the pressure correction scheme we approximate the inverse of Q_h^k at a point and the nonuniform gird poses no extra problems.

Our proposed smoother for the Navier–Stokes and continuity equations thus consists of:

(i) uncoupling and smoothing the momentum equations;

(ii) satisfying continuity via the extended pressure correction scheme of Van Doormaal and Raithby [12] which involves the solution of the pressure-correction equations (15).

4. Multigrid Scheme for the Solution of the Rotating Discs Problem

We now discuss the multigrid algorithm used, giving details of the various components.

The algorithm employs sequences of nonuniform staggered grids; the finest being defined by positioning the pressure lines to correspond with the zeros of the relevant shifted Chebyshev polynomial; clustering the grid points near the boundaries allows us to maintain accuracy without using large numbers of grid points, which would be required by a uniform grid, in order to deal with the boundary layers which form both on the discs and at the source and sink. The radial and axial velocity lines are positioned halfway between pressure lines. The grid coarsening was done by taking every other fine grid pressure lines as a coarse grid pressure line, with the coarse grid radial and axial velocity lines halfway between coarse grid pressure lines. The aim of maintaining coarse grid lines adjacent to the boundaries is to avoid the necessity for special handling of coarse grid boundary conditions.

A FAS algorithm was used in a form where the stage at which transfer occurs between grids is fixed in advance (referred to as a cycling algorithm [1]). This type of algorithm is characterised by the following four parameters:

ν_b, the number of relaxation sweeps before coarse grid correction;

ν_a, the number of relaxation sweeps after coarse grid correction;

ν_c, the number of relaxation sweeps on the coarsest grid;

γ, the number of iterations of the multigrid algorithm for the coarse grid equation ($\gamma = 1$ gives V-cycles, $\gamma = 2$ gives W-cycles, see [1, 11]).

Detailed descriptions of various multigrid algorithms can be found in Stüben and Trottenberg [11].

At this point we will introduce some notation which will be convenient for later use. We will use the multigrid algorithm in two modes: MG and FMG. The FMG mode is a method of producing good initial fine grid approximations by interpolation of a coarser grid solution produced by a similar FMG process; whereas the MG mode uses a guessed solution as the initial fine grid approximation.

Let $R_1, R_2, ..., R_m$ be the sequence of grids, with R_1 the finest grid; denote by MG_i one multigrid iteration starting on R_i. Then we denote by

$$\mathrm{FMG}(is, n_{it}) \tag{16}$$

the FMG mode of the multigrid algorithm in the following form

$$n_{it} \times \mathrm{MG}_l, \qquad l = is, is-1, ..., 2$$

followed by MG_1; i.e., n_{it} multigrid iterations on grids R_{is}, $R_{is-1}, ..., R_2$, followed by one multigrid iteration on the finest grid. Interpolation of the solution on grid R_l is used as the initial approximation on the grid R_{l-1} ($l = is, is-1, ..., 2$). If $is = m$ we start this process by a fixed number, ν_m, of relaxation sweeps on the coarsest grid.

Solution of the rotating discs problem was by either $n \times \mathrm{MG}_1$ or by $\mathrm{FMG}(is, n_{it}) + n \times \mathrm{MG}_1$, for some is, n_{it}, where n represents repeated multigrid iterations until convergence to a prescribed tolerance is achieved. As the magnitudes of the variables vary greatly the convergence criterion was based on relative rather than absolute changes. The root-mean-square (rms) was used to measure the variables and the changes made to the variables across the grid, the iteration being terminated when rms(change)/rms(variable) was less than 1.0×10^{-4} for all four variables.

The relaxation method used was the extended pressure correction scheme of Van Doormaal and Raithby [12] as in Section 3. The solution of the momentum equations was by one alternating line Gauss–Seidel (ALGS) sweep per equation; the pressure correction equations were solved by the use of 3 ALGS sweeps.

Transfer from fine to coarse grids was by full weighting restriction operators, following [4], which use a weighted average of all neighbouring fine grid points to transfer the variables and defects to the coarse grid. Simpler forms of restriction operators are given in [11]. For the nonuniform staggered grids and grid coarsening as described above these were modified from the standard operators used for uniform grids.

The interpolation of coarse grid corrections was by bilinear interpolation and the interpolation of initial approximations in the FMG process was by either bilinear or cubic interpolation (we make a comparison of the effect of the two in Section 5).

Initial solutions were as for solid body rotation, i.e., $u = v = w = p' = 0$; though in the FMG process these will be taken on a coarser grid. The nonlinearity of the equations forces underrelaxation, which is implemented as in Lonsdale and Walsh [7]. We also use the term introduced by Gosman *et al.* [5]

$$\alpha \frac{\rho}{r}(\Omega r + v)(u_{\text{old}} - u_{\text{new}}) \tag{17}$$

added to the radial momentum equation. The inclusion of this term improves the handling of the coupling of the radial and tangential momentum equations and is discussed in detail in [7]. Provision was made for different values of α in (17) to be taken on the various grids in the multigrid process; in the next section we discuss numerical tests to discover the best strategies for the choice of α.

5. Numerical Results

In this section we consider the behaviour of the nonlinear multigrid algorithm described in Section 4 applied to the test case of Section 1 at rotation rates $\Omega = 1.0$ and 10.0 (i.e., rotational Reynolds numbers of approximately 2.5×10^3 and 2.5×10^4). For the case $\Omega = 1.0$, Chebyshev grids of sizes 17×17, 33×33, and 65×65 were used as finest grids. For the $\Omega = 10.0$ case only the 33×33 and 65×65 grids were used as the finest. The reason for this is that the 17×17 grid cannot accurately represent the flow field for the higher rotation rate which leads to much narrower boundary layers.

While "optimum" values of α in (17) may be found for each grid in the multigrid process, obtained by extrapolation from those found in Lonsdale and Walsh [7], numerical experiments have shown that it is more efficient to use a fixed value of α corresponding to one of the coarse grids. For the rotation rate $\Omega = 1.0$ we thus use $\alpha = 25.0$ and for the rotation rate $\Omega = 10.0$ we use $\alpha = 100.0$, corresponding to the "optimum" values for the 17×17 grid.

Comparisons of the two methods of solution, FMG(is, n_{it}) + nMG as opposed to nMG (see Section 4 for notation), were undertaken at both rotation rates for the grids given above and for a variety of number of grids and values of is, n_{it} and with both bilinear and cubic interpolation in the FMG process. The multigrid algorithms used were given by $\nu_b = \nu_a = 2$, $\nu_c = 3$, $\gamma = 1, 2$. While the use of the FMG mode rather than the MG mode of the multigrid algorithm can give large gains in efficiency for a simple linear problem [1, 6, 11] the gains in efficiency obtained by the use of the FMG mode for the solution of the rotating discs problem, at the rotation rates $\Omega = 1.0$, 10.0, were marginal or none. The use of cubic rather than bilinear interpolation in the FMG process did not significantly improve matters. In all cases, except for the $\Omega = 1.0$ case with finest grid 17×17, the use of the FMG mode did not reduce the number of multigrid iterations on the finest grid, even when the initial fine grid approximation was interpolated from a converged coarse grid solution. The reason for the failure of the FMG mode to

improve on the convergence probably lies in the coupling of the equations and on the fact that we are forced to use separate interpolation schemes for each of the variables due to the nonuniform staggered grids; for example, while continuity may be satisfied on the coarse grid the interpolations may lead to fine grid variables which are far from satisfying continuity on the fine grid.

We thus take as our solution procedure the repeated multigrid iterations starting on the finest grid.

In giving the results we use two estimates of the computational costs in order to reflect the two situations of restricted or unrestricted storage (see Lonsdale [8]). The work units are based on the number of arithmetic operations per point required by one double sweep of the ALGS algorithm calculated assuming unrestricted storage (the work units for all operations in the algorithm are given in Lonsdale [8]). The CPU times give a measure of the computational cost when storage is limited.

Table I gives the best performance of the method for the $\Omega = 1.0$ case, together with the value of the underrelaxation parameter for the pressure correction, β, and the number of grids used. In all cases the parameters of the algorithm were: $\gamma = 1$, $\nu_b = \nu_a = 2$, $\nu_c = 3$.

Table I shows the type of behaviour that we aim for in using a multigrid algorithm.

If N is the number of points in the finest grid then the work required to obtain convergence is not far from $O(N)$ (recall that the work units for each grid are based on the number of operations per point for that grid). This shows up very clearly when comparing the nonlinear multigrid algorithm with the best of the pressure correction methods of Lonsdale and Walsh [7], the extended method of Van Doormaal and Raithby, with and without the use of a linear multigrid solver for the pressure correction. Table II gives a comparison of the two methods for the $\Omega = 1.0$ case, where we use the following abbreviation:

pc-3 ALGS — Van Doormaal and Raithby's extended pressure correction method using 3 ALGS sweeps for the pressure correction;

pc-MG — the extended pressure correction method using a linear multigrid solver;

NMG — nonlinear multigrid algorithm.

TABLE I

Performance of the Nonlinear Multigrid Algorithm with $\Omega = 1.0$

Finest grid	Number of grids used	β	Approximate work units per point	CPU s (CDC 176)
17×17	3	1.0	720	6.2
33×33	3	0.7	810	27.4
65×65	5	0.4	1190	179.4

TABLE II

Comparison of the Extended Pressure Correction Method with the Nonlinear Multigrid Algorithm with $\Omega = 1.0$

Finest grid	Method	Approximate work units per point	CPU s (CDC 176)
17×17	pc-3 ALGS	1200	11.3
	pc-MG	1010	9.4
	NMG	720	6.2
33×33	pc-3 ALGS	2940	112.5
	pc-MG	2160	78.0
	NMG	810	27.4
65×65	pc-3 ALGS	> 7380	> 1261.8
	pc-MG	4350	724.8
	NMG	1190	179.4

The ">" signs in the pc-3 ALGS results for the 65×65 grid are due to the fact that convergence had not quite been achieved.

Table II shows a large gain in efficiency in using the nonlinear multigrid algorithm—a gain in efficiency which increases as the grid is refined—giving savings for the 65×65 grid of over 72% when compared to pc-MG and over 83% when compared to pc-3 ALGS.

The nonlinear multigrid algorithm was then used for the rotation rate $\Omega = 10.0$. As we have mentioned previously, this problem involves much thinner boundary layers than the $\Omega = 1.0$ case and so we do not use the 17×17 grid as the finest grid of a multigrid procedure. In solving the $\Omega = 10.0$ case the work required to obtain convergence is greatly increased from that required for the $\Omega = 1.0$ case. The convergence history at the two rotation rates for the 65×65 grid is illustrated in Figs. 1 and 2. Figure 1 clearly shows that the convergence rate for the axial momentum equation is unaltered as Ω is increased, while Fig. 2 shows that for the tangential momentum equation the convergence rate alters with Ω. The reason for this is that the axial velocity is affected by the increased rotation rate far less than the radial and tangential velocities (the radial momentum equation convergence history being similar to that of the tangential momentum equation shown in Fig. 2). From Fig. 2 we can see that the use of the zero initial approximations gives a much larger initial defect which together with some degradation in the convergence rate explains the increased work to obtain convergence for the $\Omega = 10.0$ case.

Table III gives the best performance of the method for the $\Omega = 10.0$ case together with the values of β and the number of grids used. For the 65×65 grid we use multigrid parameters: $\gamma = 1$, $\nu_b = \nu_a = 2$, $\nu_c = 3$; however, for the 33×33 grid it was found to be slightly more efficient to use $\gamma = 1$, $\nu_b = \nu_a = 5$, $\nu_c = 10$.

While the work units and CPU times are increased from those in Table II we

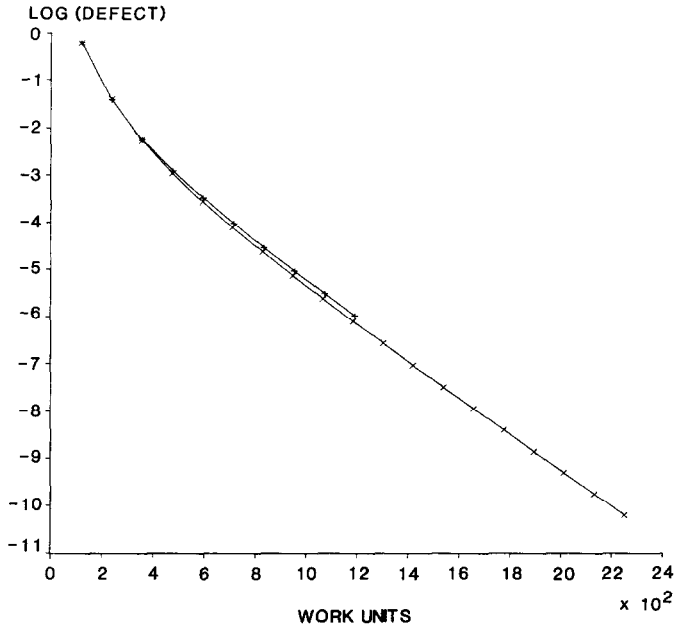

FIG. 1. Convergence history for the axial momentum equation, 65×65 grid; rotation rate $\Omega = 1.0$ (+); $\Omega = 10.0$ (×).

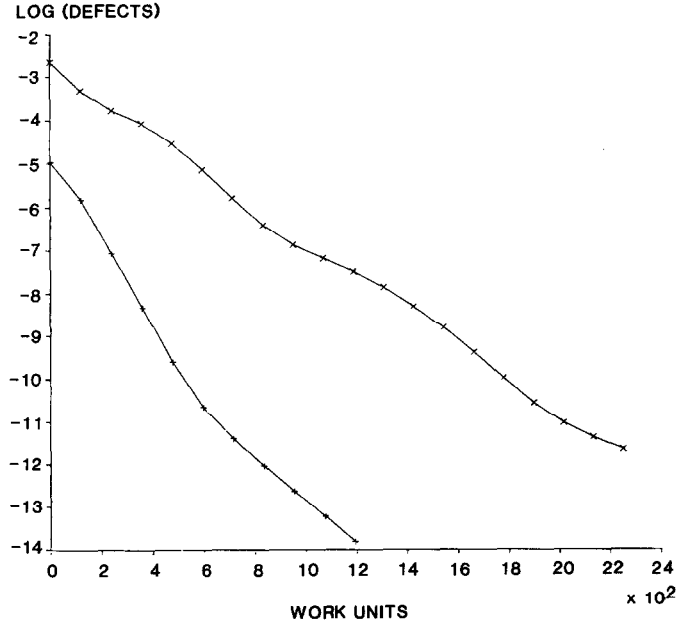

FIG. 2. Convergence history for the tangential momentum equation, 65×65 grid (same rotation rates as Fig. 1).

TABLE III

Performance of the Nonlinear Multigrid Algorithm with $\Omega = 10.0$

Finest grid	Number of grids used	β	Approximate work units per point	CPU s (CDC 176)
33×33	3	0.5	2330	83.5
65×65	4	0.4	2250	337.9

note that we still have the same order of improvement over the pc method; for example, with the 33×33 grid using pc-MG we get convergence in approximately 5780 work units, 214.5 s CPU time. We also note that we again get convergence in an amount of work proportional to the number of grid points.

Convergence was reached at the higher rotation rates of $\Omega = 30.0$, 40.0, and 50.0 (coreresponding to rotational Reynolds numbers of approximately 7.4×10^4, 1.0×10^5, and 1.25×10^5) but the increase in computing time prevented extensive numerical testing.

6. Conclusions

In Section 3 the extended pressure correction scheme of Van Doormaal and Raithby [12] was analysed as a smoother for the Navier–Stokes and continuity equations and advantages in using the pressure correction scheme were discussed. The scheme was successfully implemented as the smoother of a nonlinear multigrid algorithm for the solution of the problem of laminar, source-sink flow between corotating discs, giving much improved convergence rates in comparison with what is viewed to be an efficient one-grid method (which included the use of a linear multigrid algorithm in part of the solution process). The convergence in a computational cost proportional to the number of grid points was achieved. While the method shows some deterioration of convergence rate with increasing Reynolds number, the level of improvement over the one-grid method remains the same.

An important feature concerning the possible implementation of a major production code is the use of a pressure correction technique using nonuniform grids; so that a nonlinear multigrid method could be constructed around an existing code, providing the geometry is not too complicated.

The algorithm described is applicable to laminar flows, it remains to be seen whether or not the ideas can be suitably modified to provide an algorithm for turbulent flow calculations. In future work it is intended to consider extensions of the algorithm described here and also to make a comparison between this and various other multigrid schemes which have been put forward for the solution of the Navier–Stokes equations [2, 4, 13, 14].

ACKNOWLEDGMENTS

The author gratefully acknowledges the support of the Science and Engineering Research Council and of Rolls-Royce Ltd., Derby (through the C.A.S.E. Scheme).

REFERENCES

1. A. BRANDT, *Multigrid techniques: 1984 guide with applications to fluid dynamics* (GMD-Studien 85, Bonn, 1984).
2. A. BRANDT AND N. DINAR, "Multigrid solutions to elliptic flow problems," *Numerical Methods for Partial Differential Equations*, edited by S. V. Parter (Academic Press, New York, 1979), p. 53.
3. J. W. CHEW, *Int. J. Numer. Methods Fluids* **4**, 667 (1984).
4. L. FUCHS AND H. S. ZHAO, *Int. J. Numer. Methods Fluids.* **4**, 539 (1984).
5. A. D. GOSMAN, M. L. KOOSINLIN, F. C. LOCKWOOD, AND D. B. SPALDING, "Transfer of heat in rotating systems," ASME Paper 76–GT–25, Gas Turbine and Fluid Eng. Conf., New Orleans, LA, March 21–25, 1976.
6. G. LONSDALE, M. Sc. thesis, Manchester University, 1983 (Unpublished).
7. G. LONSDALE AND J. E. WALSH, Acceleration of the pressure correction method for a rotating Navier–Stokes problem, submitted for publication.
8. G. LONSDALE, Numer. Anal. Tech. Rept. 105, Manchester University, 1985 (unpublished).
9. S. V. PATANKAR, *Numerical Heat Transfer and Fluid Flow* (Hemisphere, Washington, DC/New York, 1980).
10. S. V. PATANKAR AND D. B. SPALDING, *Int. J. Heat Mass Transfer* **15**, 1787 (1972).
11. K. STÜBEN AND U. TROTTENBERG, in *Multigrid Methods, Proceedings Köln–Porz*, 1981, edited by W. Hackbusch and U. Trottenberg (Springer–Verlag, Berlin, 1982), p. 1.
12. J. P. VAN DOORMAAL AND G. D. RAITHBY, *Numer. Heat Transfer* **7**, 147 (1984).
13. S. P. VANKA, *J. Comput. Phys.* **65**, 138 (1986).
14. S. P. VANKA, *Int. J. Numer. Methods Fluids* **6**, 459 (1986).
15. R. S. VARGA, *Matrix Iterative Analysis* (Prentice–Hall, Englewood Cliffs, NJ, 1962).